Experimental Report

20/02/2014

Proposal: **1-01-135** **Council:** 10/2012

Title: Internal stresses after welding for age hardening materials: advancedmodelisations vs neutrons characterizations

This proposal is a new proposal

Research Area: Materials

Main proposer: **BARDEL Didier**

Experimental Team: BARDEL Didier
PANCHENG shao

Local Contact: PIRLING Thilo

Samples: AA6061

Instrument	Req. Days	All. Days	From	To
SALSA	10	5	27/03/2013	01/04/2013

Abstract:

Welding process induced in the heat affected zone (HAZ) and in the molten zone various complex phenomena: cyclic loading, miscrostructural evolutions, fluid flow within the weld pool, etc... In many key industries such as transportation (aerospace, automotive…) and energy (nuclear) the prediction of residual stresses after welding is a challenge to know the service life of key components. To achieve this goal, the finite element (FE) method [1] is often used.
Many commercial packages such as Abaqus, Code_Aster or Sysweld may be used to simulate the welding process. However when coupling between thermomechanical and microstructural effects is required as for age hardening materials, but the current FE models are not satisfactory. In fact, several phenomena that can occur in the HAZ are not classically considered: precipitates can nucleated, growth, coarse and dissolve [2][3][4][5]. These evolutions induce important differences on the mechanical behavior: during welding hardening or softening may occur, depending on the precipitation kinetics which is linked to the temperature history [3][4][5][6]. So a coupled approach (microstructural/mechanical) must be used to model the HAZ.

Experimental report: Internal stresses after welding for age hardening materials: advancedmodelisations vs neutrons characterizations

D. Bardel[e,b], D. Nelias[e,*], V. Robin[c], T. Pirling[f], X. Boulnat[b], M. Perez[b,**]

[a] *Universite de Lyon, INSA-Lyon, LaMCoS UMR CNRS 5259, F69621 Villeurbanne, France*
[b] *Universite de Lyon, INSA-Lyon, MATEIS UMR CNRS 5510, F69621 Villeurbanne, France*
[c] *AREVA NP, Departement d'ingenierie mecanique, Lyon, France*
[d] *Institut Laue Langevin, F-38042 Grenoble, France*
[e] *Universite de Lyon, INSA-Lyon, LaMCoS UMR CNRS 5259, F69621 Villeurbanne, France*
[f] *Institut Laue Langevin, F-38042 Grenoble, France*

Abstract

From an article that will be soon submitted. Here some experimental results are shown and the context is roughly presented.

1. Neutrons diffraction at SALSA

A recent review presented in [1] gives an overview of the various methods to estimate the residual stresses. Here, our choice focuses on Neutrons Diffraction (ND) that can scan easily welded plates through the thickness while having an interesting resolution.

To get least biased possible residual strains, the ND were performed in the Laue Langevin Institut (ILL) in Grenoble on the SALSA instrument [2]. This device uses a high neutrons flux and the measurements are not much affected by the background noise that is low on this instrument [3]. SALSA is a neutrons diffraction instrument designed for the determination of strains $\epsilon = (d_{hkl} - d^0_{hkl})/d^0_{hkl}$ thanks to an accurate measurement of the inter-reticular distances d_{hkl} which plays the role of gauge deformation for a material under stresses [4].

When a neutron flux is projected onto a material, each neutron is diffused by the atoms of the target, these neutrons cause interference between them. For an orderly crystal we get builder interference for 2θ angles by respect to the Bragg's law:

$$n.\lambda = 2.d_{hkl}.sin\,(\theta) \qquad (1)$$

To deduce from 2θ the average inter-reticular distance d_{hkl} of a diffracting volume two kinds of methods are available: "polychromatic time of flight" and "monochromatic angular dispersive". The first is particularly suited for monitoring phase transformations, it consist to get a multitude of diffraction peaks and the wavelength by gotten thanks the time of flight. The second method, that is used on SALSA, is well suited to measure the macroscopic stresses: only one diffraction peak 2θ is recorded with a particular monochromatic wavelength [5] (here $approx 1.64$ Angstrom). In the case where a single diffraction peak is used, we choose for FCC alloys the (311) familly because they do not accumulate significantly inter-granular stresses during the sollicitation and therefore they have a representative behavior of the matrix [5, 4]. In addition, the 2θ peak is close to 90° that which provides a Gauge Volume (GV) that can be assimilated to a rectangular parallelepiped. From the diffraction peak, an average 2θ position on the GV is acquired and deformations or stresses can be deduced by comparison with an unstressed sample. Here, only first order stresses can be deduced: homogeneous on a grain aggregate.

2. Diffraction measurements

Generally the diffraction vector K (cf. fig. 2), which provides the measurement direction, focuses in three orthogonal directions to deduce the diagonal of the stress tensor. Here, the same approach is chosen, thus diffraction peaks are recorded in longitudinal, transverse and normal directions of our weld. Now, the choice of the GV depend on two main factors:

- the strain gradient which are expected in the structure. Here, the size of the MZ is about 0.5 mm close to weld foot. Then, a classical section 2x2 mm^2 for the GV should be avoided.
- the allocated beam time. Indeed, more the GV is low more the diffrated neutrons flux will be weak. However, to have a statistically good diffraction peak the count number on the detector has to be the highest possible.

For the measurements presented in this work, as well as the calibration/alignment step, the allocated time is 5 days for three differents plates. From the narrowness of the various zones in the weld, a $0.6x0.6$ mm^2 section was chosen for the GV in

*daniel.nelias@insa-lyon.fr
**michel.perez@insa-lyon.fr

normal and transverse directions (then the resolution is about 0.849 mm). This section being very low, the counting time to obtain a reliable diffraction peak is large ($\approx$ 30 − 40 min for one direction). In addition, to capture strain gradients, recovery measurement was chosen (see fig. 2). So it was decided to opt for a beam height of 20 mm in order to reduce the acquisition time. This dimension may seem important, nevertheless in normal and transverse directions the height of the beam coincides with the longitudinal direction of the weld joint (fig. 2). Moreover, the neutrons diffraction has been applied in the central section of the plate and we have shown that in this area the heat source has a stationary behavior. Thus we can expect a quasi homogeneous mechanical behavior for a very reasonable counting time ($\approx$ 7 min per point). In the longitudinal direction, the GV section is less restrictive but the height of the beam must remain moderate. Therefore, it was reduced to 15 mm (which is still important in this direction) and a 2x2x15 mm^3 GV was chosen (fig. 2).

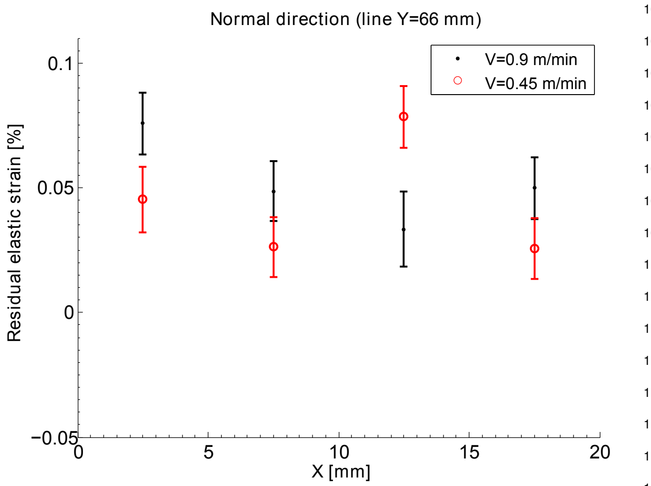

Figure 1: Example of resultats far from the weld for a plate welded with V = 0.45 m/min and V = 0.9 m/min with a raw peak reference.

The measurements gotten on the 2D SALSA detector were analyzed by using the bean line software: LAMP [6]. The diffracted intensities I are integrated to obtain an unidirectional diffraction peak (I,2θ) as show in fig. **??**. Following a correction of the background noise (a linear correction is sufficient in the presence of a sharp peak. For others peaks a noise function is deduce) a Gaussian fitting is performed and its center gives the 2θ position. In a majority of results, the error bar provided by the adjustment procedure (given by LAMP) is very low. However, in the longitudinal direction, the first measurement shown lows diffracted signals. It has been therefore decided to carry out shorter steps in this direction but with three different rotation angles ($\pm 1.5°$) for a same diffraction direction and then summed. Although a significant improvement has been noted, the quality of the diffraction signal obtained remains lower quality compared to the transverse and normal directions. This effect cannot be attributed to a texture effect, then it is probably due to a too low count time or an columnar grain influence which provides a lower amount of diffracted grains. To compensate these effects and get good quality results, a four-point moving average has been effected .

3. Residual elastic strains results

To get the residual elastic deformations $\epsilon = \Delta d_{hkl}/d^0_{hkl}$ in the material the variation of inter-reticular distance (or diffraction peak) must be performed. On SALSA, the wavelength λ can be assumed constant, then we have thanks to a Bragg's law derivate:

$$\epsilon = -\frac{\Delta 2\theta}{2.tan(\theta)} \qquad (2)$$

where $\Delta 2\theta$ is the peak displacement (from $2\theta_0$) for the same alloy without stresses and with the same local composition. Of course, this is an idealized vision because it is very difficult to satisfy these requirements in a strict way. To have a good reference value $\Delta 2\theta_0$ and to deduce $Delta 2\theta$, measurements were performed on a superposition of thin "combs" (thickness 1 mm and width 1.5 mm), which were cut from a section in the welded plate (see fig. 3). This structure allows to relax residual stresses to get a reference that best approximates a mechanical state without stresses. Then, measurements were performed in the MZ, HAZ and the BM of the combs to overcome the chemical influence. During these measurements, it was observed an expansion of the lattice from the BM to the HAZ (a dissolution of precipitates induces in the matrix a homogeneous presence of many solutes atoms) and a slight compression from the HAZ to the MZ (probably due to the smaller grain size which traps many atoms and intermetallic and therefore generates less intragranular expansion).
These references were therefore applied as a constant in the MZ and BM areas and a spline interpolation has been used in all peaks positions in the HAZ.

The first results in fig. 1 shows away from the weld (distance about 66 mm) that the residual deformations are not zero in the Base Metal. This effet can be caused by rolling process but also by a non-zero stress state in the reference combs (cf. fig. 3). The numerical simulations presented in the next section suggests that this residual strain state away from the weld must be zero. Thus, a weak shift on the diffraction peak (0.5% of the current value) was performed to have in average 0% far from the weld.

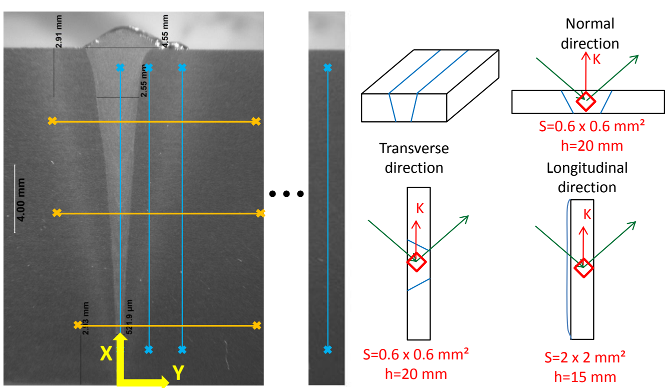

Figure 2: (a) Illustration of measured points and (b) representation of the several Gauge Volume for each orientations.

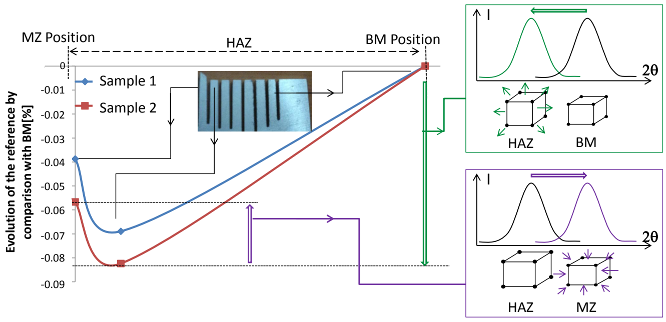

Figure 3: Combs used for the reference and representation of the chemical effect on the peak position 2θ.

Now, the figs. 4, **??** and **??** show the results of residual elastic strains in three different directions for two plates: $V = 0.45$ m/min and $V = 0.9$ m/min (the results for the plate $V = 0.72$ m/min are not show because they are between the two others). It is important to note that the error bars presented in these figures represent only the error caused by the adjustment procedure and not the various possible sources of errors. Indeed, it is just the fitting error provided by LAMP software. So it does not take into account these uncertainties: (i) eventual defects in alignment, (ii) microstructure "defects", (iii) error caused by the instrumental resolution, and (iv) inaccuracies during reference measurement (potentially a complex state of residual stresses in the comb).

In view of the results on the transverse lines (measurements in the thickness direction are not presented), one can first be satisfied with a relative good symmetry on both sides of the weld center. Then, the strain amplitudes are close to zero in the normal direction, except in the vicinity of the HAZ-BM transition. In the longitudinal direction, the strain is near zero away from the HAZ and it increases progressivly close to the MZ and then decreases in the center. Finally, for the transverse direction, we have a weak compression state in the weld center which becomes a tension state in the HAZ-BM border and then decline close to zero far away.

These results are close to the behavior observed during the laser welding process of thin plates gotten thanks to finite element simulations for a 6056 aluminum alloy [7].

4. Residual stresses estimation

Strain measurement have been carried out in three orthogonal directions in several areas of the weld. This choice allows to obtain an estimation of residual stresses amplitude in the material. In fact, by using the Hooke's law it is possible to get the diagonal of the stresses tensor σ_{ij} with the elastic Lame coefficients (λ, μ) thanks to longitudinal, transverse and normal residual strain experiments $\sigma_{ij} = \lambda\epsilon_{kk}\delta_{ij} + 2\mu\epsilon_{ij}$. In this case, the shear components cannot be determined.

It should be noted that this step (the summation by Hooke's law) does not occur without source of mistakes: (i) the using of Lame coefficient with the (311) strains neglect the anisotropy of the FCC structure [5], (ii) the summation mixte unaccurate measurements (here longitudinal) with accurates ones and then all σ_{ii} components are impacted by the worse direction, (iii) furthermore we sum results with two different resolutions and dissimilar GV. This is why, in this work, only the residual elastic strains are compared in fig. 4 to the simulations.

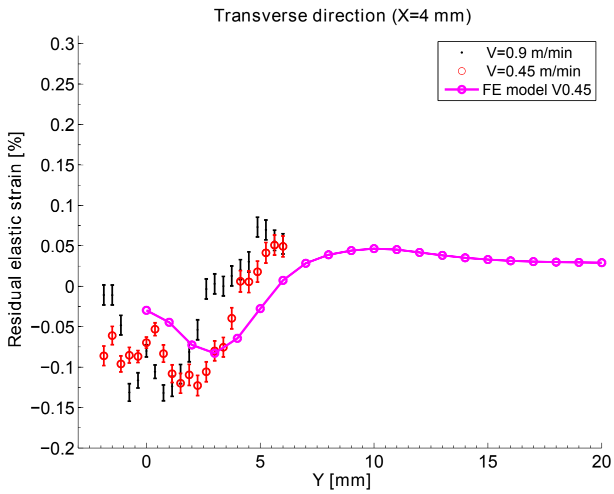

Figure 4: Residual elastic deformation for a transverse weld line at 4 mm from the lower surface for the transverse direction. Confrontation between numerical and experimental results for a welding velocity of $V = 0.45$ m/min. Additionnal experimental results are shown with $V = 0.9$ m/min to quantify the velocity influence.

References

[1] N. Rossini, M. Dassisti, K. Benyounis, A. Olabi, Methods of measuring residual stresses in components, Materials and design 35 (2012) 572–588.

[2] T. Pirling, G. Bruno, P. Withers, SALSA: advances in residual stress measurement at ILL, Materials Science Forum 524–525 (2006) 217–222.

[3] C. Acevedo, A. Evans, A. Nussbaumer, Neutron diffraction invectigations on residual stresses contributing to the fatigue crack growth in ferritic steel tubular bridges, International Journal of Pressure Vesselsand Piping 95 (2012) 31–38.

[4] J. Drezet, T. Pirling, C. Jaquerod, Residual stresses in as-cast billets: neutron diffraction measurement and thermomechanical modeling, in: Light Metals 2012 Edited by: Carlos E. Suarez, 2012.

[5] P. Withers, Mapping residual and internal stress in materials by neutron diffraction, C.R. Physique 8 (2007) 806–820.

[6] www.ill.eu/instruments-support/computing-for-science/cs-software/all-software/lamp/.

[7] M. Zain-Ul-Abdein, D. Nelias, J. Jullien, D. Deloison, Prediction of laser beam welding-induced distortions and residual stresses by numerical simulation for aeronautic application, journal of materials processing technology 209 (2009) 2907–2917.